ASTFE American Society of Thermal and Fluids Engineers

7th Thermal and Fluids Engineering Conference (TFEC)
May, 16–18, 2022
Partially Online Virtual and in Las Vegas Conference

TFEC-2022-40936

FALKNER-SKAN SIMILARITY FLOW SOLUTIONS SUBJECT TO WALL CURVATURE AND PASSIVE SCALAR TRANSPORT

Miguel Ramirez[1] and Guillermo Araya[1,*]

[1]High Performance Computing and Visualization Laboratory, Department of Mechanical Engineering.
University of Puerto Rico, Mayaguez, Puerto Rico 00681

ABSTRACT

The laminar boundary layer of a viscous incompressible fluid subject to a two-dimensional wall curvature is evaluated. It is well known that a curved surface induces streamwise pressure gradient as well as wall-curvature driven pressure gradient. Under certain assumptions, a family of similarity solutions can be obtained under the influence of flow acceleration/deceleration, which is known as the Falkner-Skan similarity solutions. In this study, the effect of the wall normal pressure gradient is taken into consideration, and the freestream flow parameters are adjusted for flow over a curved surface. Present results are obtained by numerical solution of a generalized Falkner-Skan equation governing similar solutions for flows over curved surfaces. The Falkner-Skan equations are solved by an RK4 shooting algorithm. Additionally, the transport of a passive scalar is incorporated in the present analysis at different Prandtl numbers. The objective of this paper is to use the curvilinear or axisymmetric boundary layer and energy equations to assess the effect of Favorable, Adverse and Zero pressure gradient on the laminar momentum and thermal boundary layer development. Major conclusions are summarized as follows: (i) as the pressure gradient β increases from negative values (APG) towards positive (FPG) values, the displacement (Δ^*) and momentum (θ^*) thickness tend to decrease no matter the curvature type, and, (ii) the normalized wall shear stress (i.e., f'') exhibits a linear decreasing behavior as the wall curvature switches from concave (negative) to convex (positive) at a constant pressure gradient.

KEY WORDS: Falkner-Skan, wall curvature, concave/convex surface, adverse/favorable pressure gradient, passive scalar.

1. SOME BACKGROUND

it is well-known that the Navier-Stokes (NS) equations are the foundation of the modern fluid dynamic theory [7]. These equations are used to describe the transport phenomena of momentum and its velocity-pressure field. In junction with the energy equation, these equations can be used to describe the flow with the effects wall heating and cooling. The situations where analytical solutions of the NS equations are rather limited due to its complexity and high non-linearity. However, there are several analytical (or quasi-analytical) solutions to these equations by using different assumption or simplifications for some special cases such as the Couette, Poiseuille and boundary layer problems (based on the Prandlt's theory) in laminar flows. These assumptions significantly reduces the level of complexity of the NS equations. *This paper focuses on the solution of NS for laminar boundary layers over curved surfaces.*

The boundary layer theory assumes that the velocity component parallel to the wall possesses a much larger

*Corresponding and Guillermo Araya: araya@mailaps.org

magnitude that that of the wall-normal fluid velocity component. In addition, it is assumed that the pressure perpendicular to the wall remains constant and wall-normal flow gradients are dominant with respect to streamwise flow gradients [9]. Applying these assumptions as stated before reduces the NS equations to the boundary layer equations which can be solved via a similarity analysis procedure. Generally speaking, in this methodology the x (streamwise) and y (wall-normal) coordinates are normalized via a coordinate η which in turn is considered the similarity variable. The variable η absorbs the $x-$dependency of the flow parameters, transforming the boundary layer equations to a one-dimensional problem. In this way, a high-order ordinary differential equation (ODE) is obtained that can be solved by means of a shooting method and the Runge-Kutta fourth Order (RK4) algorithm.

In boundary layer theory, a more general solution is that of a curved surface, which at the end can be approximated to a flat plate surface by prescribing an infinite curvature radius. As seen in Figure 1, the x coordinate is parallel to the surface and the y coordinate is perpendicular to the local surface. The Λ parameter is defined as $1/R$ and is called the surface curvature. Finally, the corresponding boundary layer equations can be reduced to a one dimensional problem with a fourth order ODE via a similarity analysis. It is important to mention that the boundary layer equations for curved surfaces are only applicable if the boundary layer thickness is much smaller than the local radius (i.e., $\delta(x) << r_0$). Also, it can be seen in figure 1 the velocity component parallel to the wall, u, and the wall-normal component v [7]. For the thermal transport equation (energy equation), the dissipation term must be taken in to account in high-speed flows and very high viscous fluids as well as the variation of fluid viscosity and density (via the state equation). For moderate and low viscous flows the dissipation term can be neglected. In the case of incompressible flow, the energy equation is decoupled from the momentum equation if buoyancy is neglected. Therefore, a similar procedure can be applied to the energy equation to obtain the passive scalar transport equation, and eventually, a similarity solution can be obtained for laminar boundary layers. As stated before, this similarity solution is a linear second order ODE which is solved after knowing the velocity field distribution [10].

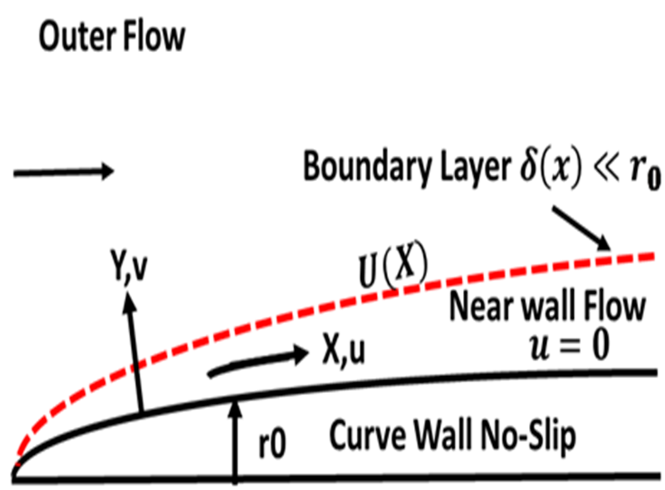

Fig. 1 Curved surface coordinates setup.

The main difficulty when solving curvature surfaces is the fact that in the boundary layer the geometry of the curvature needs to be taken in to account. Thus, the curvature indeed affect the boundary layer in contrast to the flat plate. Several research works have been done in this area. Murphy [5] investigated the effects of surface curvature on the laminar boundary layer flow for large and moderate wall curvatures for zero pressure gradient (ZPG) flows. Murphy [5] concluded that for equal Reynolds numbers the shear stresses on convex surfaces are lower than those of the concave and flat surfaces, in that order of strength hierarchy. He also stated that the smooth transition from the viscous flow to the outer flow causes the velocity profile to have a negative slope near the outer edge for the convex case, whereas, a positive slope for the concave case. Mahmood *et* *al.* [4] studied the similarity solutions of axisymmetric mixed convection boundary layer flow involving a buoyancy parameter α and a curvature parameter β and found that for large values of α and β of $O(1)$ an asymptotic solution is reached; and that for large β of O(α1/4) the problem becomes independent of the mainstream, obtaining a free convection limit. Saikrishman *et al.* [6] investigated non-similar axisymmetric water boundary layers with variable Prandtl numbers and fluid viscosity for forced convection flow over a rotating sphere up to the point of flow separation. They observed that the viscosity and Prandtl number effects caused a displacement of the separation point downstream, while the rotation parameter had a reverse effect. Saikrishman *et al.* also concluded that the heat transfer rate depended strongly on the viscous dissipation, but the skin friction coefficient was unaffected by it. Maddox [3] studied the application of the Mangler transformations to a special class of power law bodies and stated that the Mangler transformations could be used to study the laminar shear stresses and heat transfer. Ko [2] calculated the local heat-transfer coefficient of slender surfaces of revolution by the Mangler transformation. He stated that for laminar boundary layers the velocity and temperature profiles, momentum and displacement thickness, and wall shear stress can be evaluated using the Mangler transformations. Furthermore, in his paper Ko [2] extended the Mangler transformations to evaluate the heat transfer coefficient to three-dimensional faces of revolution in axisymmetric flow.

The principal objective of this paper is to study the effect of the pressure gradient (i.e., streamwise and wall-curvature-driven pressure gradients) on laminar boundary layers as well as the passive scalar transport by considering several Prandlt numbers via a similarity flow solution.

2. MATHEMATICAL EQUATIONS

2.1 Governing Equations

According to Goldstein [1] the NS governing equations for curved surfaces are as follows:

Continuity:

$$\frac{\partial u}{\partial x} + \frac{\partial}{\partial y}(1+\Lambda y)v = 0 \tag{1}$$

X-Momentum

$$\begin{aligned}\frac{\partial y}{\partial t} + \frac{1}{(1+\Lambda y)}u\frac{\partial u}{\partial x} + v\frac{\partial u}{\partial y} + \frac{\Lambda}{(1+\Lambda y)}uv = \frac{-1}{\rho}\frac{1}{(1+\Lambda y)}\frac{\partial P}{\partial x} + \nu\Bigg[\frac{1}{(1+\Lambda y)^2}\frac{\partial^2 u}{\partial x^2} \\ + \frac{\partial^2 u}{\partial y^2} - \frac{1}{(1+\Lambda y)^2}\frac{\partial \Lambda}{\partial x}\frac{\partial u}{\partial x} + \frac{\Lambda}{1+\Lambda y}\frac{\partial u}{\partial y} - \frac{\Lambda^2}{(1+\Lambda y)^2}u + \frac{1}{(1+\Lambda y)^3}\frac{\partial \Lambda}{\partial x}v + \frac{2\Lambda}{(1+\Lambda y)^2}\frac{\partial v}{\partial x}\Bigg]\end{aligned} \tag{2}$$

Y-Momentum

$$\begin{aligned}\frac{\partial v}{\partial t} + \frac{\Lambda}{1+\Lambda y}u\frac{\partial v}{\partial x} + v\frac{\partial v}{\partial y} - \frac{\Lambda}{1+\Lambda y}u^2 = \frac{-1}{\rho}\frac{\partial P}{\partial y} + \nu\Bigg[\frac{1}{(1+\Lambda y)^2}\frac{\partial^2 v}{\partial x^2} \\ + \frac{\partial^2 v}{\partial y^2} - \frac{y}{(1+\Lambda y)^3}\frac{\partial \Lambda}{\partial x}\frac{\partial v}{\partial x} + \frac{\Lambda}{1+\Lambda y}\frac{\partial v}{\partial y} - \frac{\Lambda^2}{(1+\Lambda y)^2}v - \frac{1}{(1+\Lambda y)^3}\frac{\partial \Lambda}{\partial x}u - \frac{2\Lambda}{(1+\Lambda y)^2}\frac{\partial u}{\partial x}\Bigg]\end{aligned} \tag{3}$$

Applying the boundary layer assumptions to equations 1, 2 and 3:

Continuity:

$$\frac{\partial u}{\partial x} + \frac{\partial v}{\partial y} = 0 \tag{4}$$

X-Momentum:

$$\frac{\partial u}{\partial t} + u\frac{\partial u}{\partial x} + v\frac{\partial u}{\partial y} = \frac{-1}{\rho}\frac{\partial P}{\partial x} + \nu\frac{\partial^2 u}{\partial y^2} \tag{5}$$

Y-Momentum:

$$-\Lambda u^2 = \frac{-1}{\rho}\frac{\partial P}{\partial y} \tag{6}$$

2.2 Similarity Equations

According to Murphy [5] applying a similarity analysis to equations 1, 2 and 3 yields the following fourth order similarity equation:

$$f^{IV} + ff^{III} + \Omega[f^{III} + ff^{II}] - \gamma[f^I f^{II} + \Omega f^I f^I] = 0 \tag{7}$$

Boundary Conditions:

$$\eta = 0; f = f^I = 0 \tag{8}$$

$$\eta \to \infty; f^I = e^{-\Omega\eta}; f^{II} = -\Omega e^{-\Omega\eta} \tag{9}$$

Its important to highlight that in this analysis f is associated to the stream function, f^I is related to the streamwise velocity (parallel to the surface) and f^{II} is connected to the local shear stress inside the boundary layer.

The similarity variable used to normalize x and y is given as:

$$\eta = y\sqrt{\frac{[(m+1)/2]U_0}{\nu x}}, \tag{10}$$

the power parameter is defined as:

$$m = \frac{\gamma+1}{3-\gamma}, \tag{11}$$

the curvature parameters is:

$$\Lambda = \Omega\sqrt{\frac{[(m+1)/2]U_0}{\nu x}}, \tag{12}$$

the potential velocity U_0 is:

$$U_0 = U_\infty C_2^{(m+1)/2}\left[\frac{2}{m+1}\frac{x}{L}\right]^m, \tag{13}$$

the pressure gradient is defined as:

$$\gamma = 2\beta - 1. \tag{14}$$

The integral boundary layer parameters are:

$$\Delta^* = \int_0^\infty \left[1 - \frac{f^I}{e^{-\Omega*\eta}}\right]dx, \tag{15}$$

$$\theta^* = \int_0^\infty \left[\frac{f^I}{e^{-\Omega\eta}}\right]\left[1 - \frac{f^I}{e^{-\Omega\eta}}\right]dx, \tag{16}$$

$$H = \frac{\Delta^*}{\theta^*}, \tag{17}$$

i.e., displacement thickness, momentum thickness and shape factor, respectively

2.3 Numerical Details

Figure 2 shows an schematic of the algorithm used to solved equation 7. This method is called the point and shoot algorithm. This algorithm works as follows: first the f^{II} and f^{III} are guessed; next a Runge Kutta fourth order solver is applied to numerically compute equation 7; finally, the resulting outcomes of f^{I} and f^{II} are compared to the boundary conditions 9 in an iterative procedure.

According to the differential equations with boundary value problems book [8], the Runge-Kutta fourth order methodology is applied for a general case as:

$$Y_{n+1} = Y_n + \frac{\Delta n}{6}[K_1 + 2K_2 + 2K_3 + K_4] \tag{18}$$

$$K_1 = f(X_n, Y_n) \tag{19}$$

$$K_2 = f\left(X_n + \frac{\Delta n}{2}, Y_n + \frac{K_1 \Delta n}{2}\right) \tag{20}$$

$$K_3 = f\left(X_n + \frac{\Delta n}{2}, Y_n + \frac{K_2 \Delta n}{2}\right) \tag{21}$$

$$K_4 = f\left(X_n + \Delta n, Y_n + K_3 \Delta n\right) \tag{22}$$

The Runge Kutta algorithm is called a single step method. Equation 18 is used to update the values of f, f^{I}, f^{II} and f^{III} by taking the average of the K_1, K_2, K_3 and K_4 points. The displacement and momentum

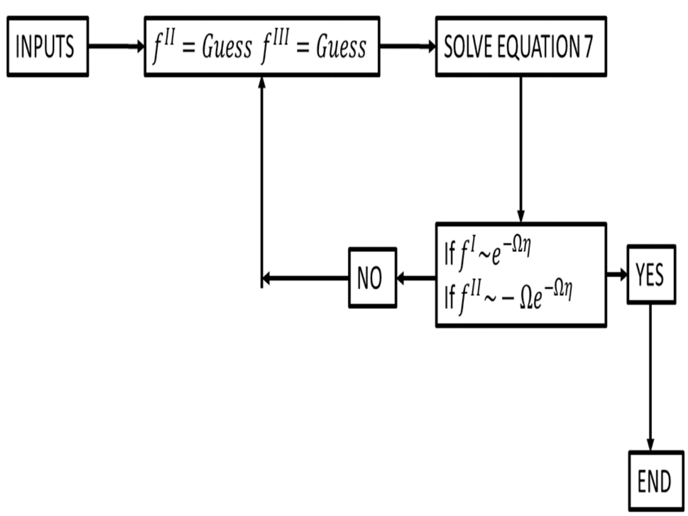

Fig. 2 Numerical algorithm setup.

thickness can be obtained via a Simpson algorithm where for a closed integral is known that:

$$\int_a^b f(x)dx = \frac{\Delta x}{3}\left[Y_{first} + 4\left(\sum Y_{odd}\right) + 2\left(\sum Y_{even}\right) + Y_{last}\right] \tag{23}$$

In this case the a and b values are the limits of the integral and the term Δx is the spacing of the points between a and b. The following linear approximations were used to estimate the $f^{II}(0)$ based on Murphy's paper Figure 4 [5] for a β equal to 1, 0.2, 0 and -0.1:

$$f^{II}(0) = -1.6426\Omega + 1.2302 \tag{24}$$

$$f^{II}(0) = -1.3003\Omega + 0.6861 \tag{25}$$

$$f^{II}(0) = -1.0189\Omega + 0.4693 \tag{26}$$

$$f^{II}(0) = -0.7359\Omega + 0.319 \tag{27}$$

In this work a total length L_η of 10 was chosen with 1000 points to accurately solve equation 7.

3. PRELIMINARY RESULTS

Figure 3 shows the variation of f^I vs. η for a pressure gradient, β, of 1 and Ω's values of -0.1, 0 and 0.1. It can be seen in the figure that for as η increases the f^I increases from zero and tends to the potential flow profile described by equation 9 where the flow velocity matches the outer potential flow velocity. As the curvature decreases from a positive (convex) to a negative (concave) value, the curves tends to move to the left, indicating a shrinking process of the boundary layer thickness. As expected, since the streamwise pressure gradient β is positive, the infringed outer pressure gradient on the flow is favorable (FPG) or flow acceleration. Additionally, the concave curvature causes (i.e., $\Omega < 0$) flow acceleration, as well, and the combined effects clearly induce a local increase of the streamwise velocity u (given by the normalized parameter f') inside the boundary layer, more obvious by the edge ($\eta \approx 2$). In particular, when the wall curvature Ω is zero, the solution is that of the Falkner-Skan flow for a flat plate in a purely accelerated flow by the outer region at $\beta = 1$.

Figure 4 shows the variation of f^{II} vs. η for a pressure gradient of 1 and Ω value of -0.1, 0 and 0.1. The second derivative of the stream function f is proportional to the local shear stress by friction in the boundary layer. It can be seen in the figure that as η increases the f^{II} sharply decreases until matching the potential flow values of f^{II}, as described by equation 9. As the curvature parameter decreases from a positive (convex) to a negative (concave) value, the shear stress at the wall increases and the final value of the f^{II} increases, as expected for highly accelerated flows. Also when the curvature parameter Ω is zero, the solution is that of the Falkner-Skan flow for a flat plate and tends to zero in the outer flow section. Figure 5 depicts the variation of f^I vs. η for $\beta = 1$, 0.2, 0, -0.1 and $\Omega = 0.1$ (convex). It can be seen in the figure that as the pressure gradient β increases the f^I tends to move leftward or reaches the potential flow condition faster (boundary layer thickness shrinks). It can also be observed that all f^I curves for all the pressure gradients match the potential flow curve beyond the boundary layer thickness since the potential flow velocity is only function of the wall curvature Ω. Figure 6 exhibits the variation of f^{II} vs η for a pressure gradient of 1, 0.2, 0, -0.1 and Ω value of 0.1 (convex). It can be seen in the figure that as the pressure gradient β increases the f^{II} at the wall increases and the wall shear stress, as well. It can also be observed that all f^{II} curves for all the pressure gradients match the potential flow curve.

Figure 7 shows the variation of f^{II} vs. Ω for pressure gradients of 1, 0.2, 0, -0.1. As stated before, it can be seen in the figure that as the pressure gradient β increases the f^{II} (and wall shear stress) at the wall increases, as well. For a β-constant profile, it can also be observed that as the Ω increases from negative to positive the $f^{II}(0)$ decreases. This means that as the curvature parameter increases or becomes more positive the $f^{II}(0)$ or shear stress at the wall decreases. As a consequence, for an imposed outer pressure gradient β, by increasing the wall curvature towards positive (convex) values the skin friction coefficient is decreased. Table 1 shows the variation of the displacement, momentum thickness and shape factor for different wall curvatures (Ω = -0.1, 0 and 0.1) and pressure gradients (β = 1, 0.2, 0 and -0.1). A fairly good agreement was achieved with numerical results of Murphy [5]. Major conclusions are summarized as follows for Δ^*, θ^*, and H: (i) at a fixed wall curvature, these boundary layer parameters increase as the pressure gradient decreases from favorable

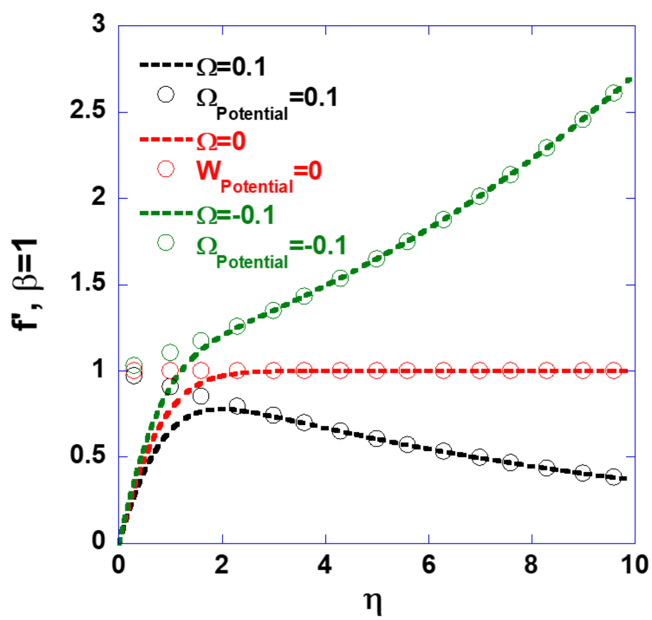

Fig. 3 f^{I} vs. η for $\beta = 1$ and Ω = -0.1, 0 and 0.1

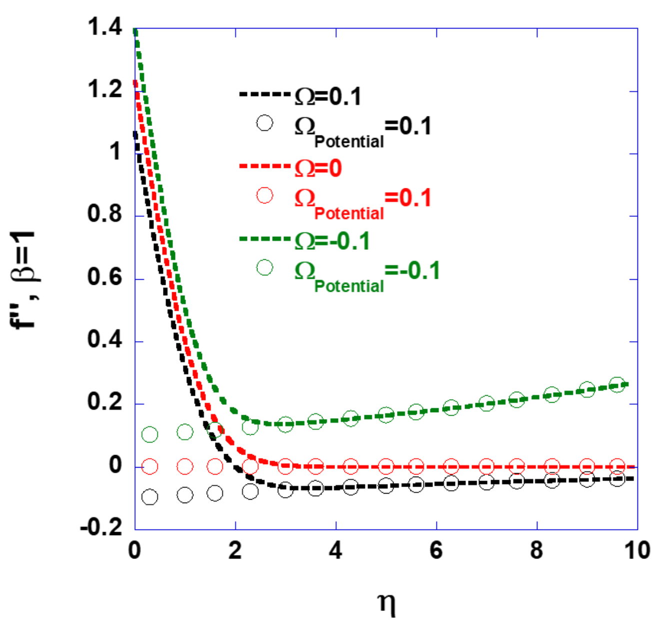

Fig. 4 f^{II} vs. η for a pressure gradient of 1 and Ω of -0.1, 0 and 0.1

(positive) to adverse (negative) values of β, and, (ii) at a fixed pressure gradient, the three parameters increase as the wall curvature switches from concave (negative) to convex (positive) values.

4. CONCLUSIONS

A similarity solution is introduced for laminar boundary layers subject to wall curvature and pressure gradients based on works by [5] and [1]. In conclusion, the curve-linear similarity solution differs from the flat plate in the sense that the geometry of the wall has to be taken into account. This can be seen in equation 6 where the wall-normal pressure is not constant nor negligible in general, as in the flat plate case but rather depends on the

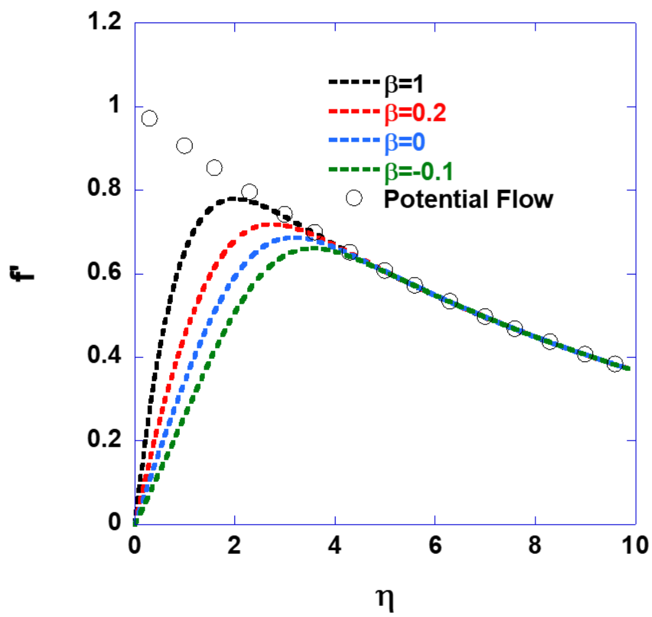

Fig. 5 f^{I} vs η for a pressure gradient of 1, 0.2, 0, -0.1 and Ω of 0.1

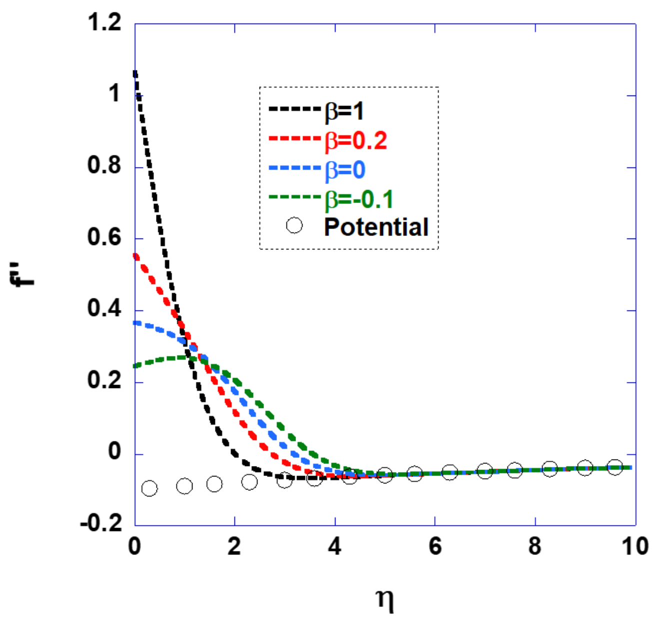

Fig. 6 f^{II} vs. η for a pressure gradient of 1, 0.2, 0, -0.1 and Ω of 0.1

Table 1 Boundary layer parameters

β	Ω	Δ^*	θ^*	**H**
1	-0.1	0.56599	0.25289	2.238087706
1	0	0.6537	0.30045	2.175736395
1	0.1	0.74299	0.33885	2.192681127
0.2	-0.1	0.84974	0.35612	2.386105807
0.2	0	0.98298	0.40982	2.398565224
0.2	0.1	1.1572	0.47365	2.443154228
0	-0.1	1.0489	0.41254	2.542541329
0	0	1.2142	0.47001	2.58334929
0	0.1	1.4468	0.54651	2.647344056
-0.1	-0.1	1.2426	0.45249	2.746138036
-0.1	0	1.4400	0.51520	2.795031056
-0.1	0.1	1.7270	0.60302	2.863918278

curvature and the local fluid speed. It was observed that as the Ω decreases or becomes negative the boundary layer thickness decreases and the shear stress of the wall increases. As the pressure gradient β increases from negative (APG) towards positive (FPG) values, the displacement and momentum thickness tends to decrease no matter the curvature type. The normalized wall shear stress (i.e., f'') exhibits a linear decreasing behavior as the wall curvature switches from concave (negative) to convex (positive) at a constant pressure gradient. Also, it was seen that for the special case of Ω equals zero in equation 7 is that of the flat plate. This shows that the curve-linear similarity solution (equation 7) is a more general solution for the Falkner-Skan equation.

5. FUTURE WORK

Next steps are summarized below:

- The temperature is going to be taken into account as a passive scalar.

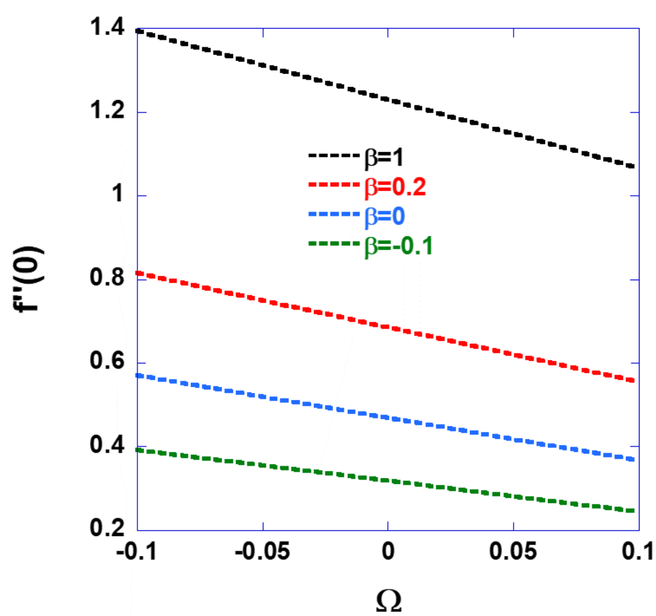

Fig. 7 $f^{II}(0)$ vs. Ω for β = 1, 0.2, 0, -0.1.

• The effect of different Prandlt numbers on the boundary layer are going to be studied.

ACKNOWLEDGMENTS

This material is based upon work supported by the Air Force Office of Scientific Research (AFOSR) under award number FA9550-17-1-0051 and the National Science Foundation under Grant No. 1847241.

NOMENCLATURE

X	rectangular coordinate parallel to the wall	(m)
Y	rectangular coordinate perpendicular to the wall	(m)
x	curvature coordinate parallel to the wall	(m)
y	curvature coordinate perpendicular to the wall	(m)
r_0	distance form the axisymetric axis to the curve wall	(m)
u	velocity component parallel to the curve wall surface	(m/s)
v	velocity component perpendicular to the curve wall surface	(m/s)
δ	boundary layer thickness	(m)
Λ	wall curvature	(m^{-1})
R	wall curvature radius	(m)
ν	kinematic viscosity	(m^2/s)
P	pressure	(Pa)
ρ	density	(kg/m^3)

η	similarity variable	(-)
Ω	curvature parameter	(-)
m	power parameter	(-)
U_0	boundary layer edge velocity	(m/s)
U_{inf}	free stream velocity	(m/s)
γ	pressure gradient parameter	(-)
β	pressure gradient	(-)
Δ^*	displacement thickness	(-)
θ^*	momentum thickness	(-)
H	shape factor	(-)

REFERENCES

[1] Goldstein, S., *Modern Developments in Fluid Dynamics an Account of Theory and Experiment Relating to Boundary Layers, Turbulent Motion and Wakes*, Oxford at the Clarendon Press, (1938).

[2] Ko, S.-Y., “Calculation of local heat-transfer coefficients on slender surfaces of revolution by the mangler transformation,” *JOURNAL OF THE AERONAUTICAL SCIENCES*, , pp. 62–63, (1958).

[3] MADDOX, A. W., “Application of the mangler transformation to a special class of power law bodies,” *AIAA JOURNAL*, 1, pp. 1186–1187, (1962).

[4] MAHMOOD, T. and MERKIN, J., “Similarity solutions in axisymmetric mixed-convection boundary-layer flow,” *Journal of Engineering Mathematics*, , pp. 73–92, (1988).

[5] MURPHY, J. S., “Extensions of the falkner-skan similar solutions to flows with surface curvature,” *AIAA JOURNAL*, 3, pp. 2043–2049, (1965).

[6] Saikrishnan, P. and Roy, S., “Steady nonsymmetric water boundary layers with variable viscocity and prandtl number,” *Acta Mechanica*, , pp. 187–199, (2002).

[7] White, F. M., *Viscous Fluid Flow*, McGraw-Hill, (1991).

[8] ZILL, D. G., WRIGHT, W. S., and CULLEN, M. R., *DIFFERENTIAL EQUATIONS with Boundary-Value Problem*, Brooks/Cole, Cengage Learning, (2013).

[9] ÇENGEL, Y. A. and CIMBALA, J. M., *FLUID MECHANICS FUNDAMENTALS AND APPLICATIONS Third Edition*, McGraw-Hill, (2014).

[10] ÇENGEL, Y. A. and GHAJAR, A. J., *HEAT AND MASS TRANSFER FUNDAMENTALS & APPLICATIONS*, McGraw-Hill, (1991).